Uniaxial stress-induced symmetry breaking for muon sites in Fe

W. J. Kossler, M. Namkung,* B. Hitti, Y. Li, and J. Kempton
Physics Department, College of William and Mary, Williamsburg, Virginia 23185

C. E. Stronach and L. R. Goode, Jr.
Physics Department, Virginia State University, Petersburg, Virginia 23803

W. F. Lankford
Physics Department, George Mason University, Fairfax, Virginia 22030

B. D. Patterson and W. Kündig
Physik-Institut der Universität Zürich, CH-8001 Zürich, Switzerland

R. I. Grynszpan
Centre National de la Recherche Scientifique, Centre d'Etudes de Chimie Métallurgique, 94400 Vitry, France
(Received 22 February 1985)

Uniaxial stress has been used on Fe single crystals to induce muon-precession frequency shifts. The frequency shift for a nominally pure Fe sample at 302 K was -0.34 ± 0.023 MHz per 100 microstrain ($\mu\epsilon$) along the $\langle 100\rangle$ magnetization axis. This corresponds to a change of magnetic field at the muon of 25.1 ± 1.6 G/100 $\mu\epsilon$. For an Fe (3 wt. % Si) single crystal, the shifts were -0.348 ± 0.008 MHz/100 $\mu\epsilon$ (25.7 ± 0.5 G/100 $\mu\epsilon$ at 300 K), and -0.279 ± 0.010 MHz/100 $\mu\epsilon$ (20.6 ± 0.7 G/100 $\mu\epsilon$ at 360 K). The agreement between the shifts for Fe and Fe (3 wt. % Si) shows the effect to be intrinsic to iron and not strongly impurity sensitive. These shifts and their temperature dependence ($1/T$) are dominated by the effect of strain-induced population shifts between crystallographically equivalent, but magnetically inequivalent sites. Their magnitudes are in good agreement with theoretical predictions by Jena, Manninen, Niemenin, and Puska and by extrapolation from calculations on Nb and V by Sugimoto and Fukai, especially if both $4T(0)$ and $1T$ sites contribute comparably.

I. INTRODUCTION

The positive muon, having a rest mass of 105 MeV, may be viewed as a light isotope of hydrogen, the electronically simplest charged impurity, which can be added to metals. There are a number of questions of fundamental interest related to μ^+ implanted in metals; these include: where does the muon reside, how does it interact with lattice atoms, and how does its presence disturb the local electronic structure in ferromagnetic crystals?

In this paper we present a study of the muon's interaction with the lattice in which uniaxial stress induces an energy difference between crystallographically equivalent but magnetically inequivalent sites in an Fe single crystal. Of the parameters measured, the precession frequency of the muon, which is proportional to the average local magnetic field is of particular interest. This local field is decomposed as

$$\mathbf{B}_\mu=\mathbf{B}_{\rm ext}+\mathbf{B}_{\rm dem}+\mathbf{B}_L+\langle\mathbf{B}_d\rangle+\mathbf{B}_{\rm HF}\ , \tag{1}$$

where $\mathbf{B}_{\rm ext}$ is the applied external field, $\mathbf{B}_{\rm dem}$ is the demagnetization field due to the finite and particular shape of the sample, and $\mathbf{B}_L$ is the Lorentz field which appears inside a spherical cavity within the sample. $\langle\mathbf{B}_d\rangle$ arises from the magnetic dipoles inside the Lorentz cavity appropriately thermally averaged over magnetically inequivalent sites, but not from the contact hyperfine interaction which is included as $\mathbf{B}_{\rm HF}$. The site correlation time is probably less than 10^{-11} s at room temperature. For a general review of the experimental and theoretical situation for muons in ferromagnetic material see, e.g., Meier[1] or Kanamori *et al.*[2]

We are interested in the change of $\mathbf{B}_\mu$ with applied uniaxial stress $\Delta\mathbf{B}_\mu$. Changes in $\mathbf{B}_{\rm ext}$, $\mathbf{B}_{\rm dem}$, and $\mathbf{B}_L$ will be shown to be small for our purposes. Two features of the hyperfine field can be considered: the change with distance, especially with respect to the nearest neighbors; and differences in hyperfine field from one magnetically inequivalent, but crystallographically equivalent site to another. The first can be estimated from the measurements of Butz *et al.*[3] for Fe under homogeneous compression. As will be seen, in Sec. III there is a small effect and will (essentially) be ignored. The second is not usually calculated since there is no clear mechanism to introduce such a difference; further this difference would be multiplied by a small factor and so is ignorable unless it is of the order of the hyperfine field itself.

The remaining terms are primarily from the displacement of the nearest-neighbor dipoles and from the changes in the thermal average, both induced by strain. By far the larger of these two is the strain-induced symmetry-breaking change in the thermal average, which may be written as

$$\Delta B_\mu = \tfrac{2}{9}(B_l - B_t)\Delta E/kT \ ,$$

where

$$\Delta E = -\left[\frac{S_{11}-S_{12}}{S_{11}}\right](P_1 - P_2)\epsilon_{100} \ ,$$

S_{ij} are the elastic compliances for Fe, P_i are the diagonal elements of the double force tensor[4] associated with the muon in Fe, $(B_l - B_t)$ is the difference in magnetic fields for the magnetically inequivalent sites, and ϵ_{100} is the strain along the $\langle 100 \rangle$ direction, which is also the magnetization axis. $(B_l - B_t)$ is essentially $\frac{3}{2}B_l$, which in turn depends strongly on lattice site, local lattice distortion, and the shape of the muon's wave function while executing its zero-point motion. The double force tensor depends on the lattice site and the muon-Fe interaction, which then determines the lattice distortion and muon wave function.

Sugimoto and Fukai[5] have considered the behavior of protons and muons in the bcc metals obtaining $P_1 - P_2$ for Nb and V.[5] We use their results below to extrapolate to Fe. We also compare to the results of Jena *et al.*,[6] who calculate the shifts one measures using the effective medium model.

Yagi *et al.*[7] use the temperature dependence of the relaxation rates Γ_2^{100} and Γ_1^{111} to suggest a different intrinsic muon motion below 40 K, and possibly preferential occupancy of the T sites (i.e., Fig. 1) at the lower temperatures and of O and T at higher temperatures. The dependence on angle between $\mathbf{B}_{\rm app}$ and $\langle 100 \rangle$ of Γ indicates a site with tetragonal symmetry, i.e., T or O or a linear combination. Hydrogen in bcc lattices typically seems to have T occupancy. Larger impurities in Fe force a lattice relaxation which is large enough to favor the O site.[8] The calculations of Sugimoto and Fukai suggest that the larger zero-point motion of the muon causes it to behave as though it were larger than the proton and hence favor the $4T(O)$ site.[5]

A perplexing feature of muon spin resonance (μSR) with Fe alloyed with small quantities of other elements or Fe with high dislocation density has been the general tendency for the magnetic field at the muon to decrease in magnitude once one has taken the magnetization changes into account.[9] The present study leads to the suggestion that internal strains are responsible for the effect.

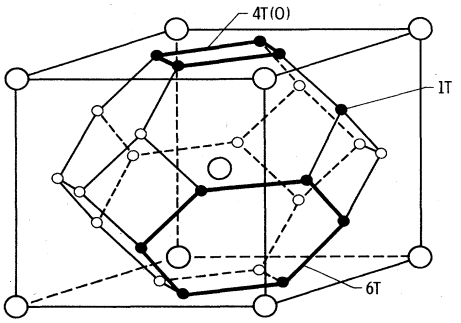

FIG. 1. Three possible occupational configurations of interstitials in a bcc crystal.

II. EXPERIMENT

A. Beam lines, μSR, and pulling apparatus

These measurements were done at the Swiss Institute for Nuclear Research (SIN) for a pure Fe single crystal, and at the alternating-gradient synchroton (AGS) of Brookhaven National Laboratory (BNL) for an Fe (3 wt. % Si) single crystal. At BNL we used beam line D2, the decay channel for stopping muons, which we, with Sachs, Fox, and Cohen, designed and had installed. The μSR apparatus there is shown in Fig. 2. For 10^{12} protons per AGS cycle on the production target we had 6000 muons through the last collimator (2.3-cm diameter) and detector M5, 1800 stops in the sample, and 350 events. Six trim coils were used to cancel residual magnetic fields and field gradients at the sample. A large Helmholtz pair, indicated in the figure, produced the aligning field. Typical asymmetries were 14%, somewhat lower than the 18% observed for nonmagnetic material. 18% corresponds in our detector geometry to about 80% polarization in the beam.

At SIN, a surface beam from the π E3 port was sent through a 2×3-mm^2 collimator of the "Mili" μSR apparatus. A positron event rate of 2000 was achieved for detectors forward and backward with respect to the beam from the sample position. A jig was used to mount the sample in order to prevent misalignment between the stress direction and the long axis of the samples. A support for the sample was used during the mounting and dismounting process to minimize extraneous mechanical strains.

Figure 3 shows the arrangement of the puller. The sample was typically held in position with epoxy. Since the epoxy was found to soften at 360 K, grooves were cut in the Fe (3 wt. % Si) sample which mated to ridges in the holder.

The sample holder assembly was insulated by a vacuum jacket. For the pure Fe sample, 302 K was maintained by circulating ethanol at a carefully controlled temperature through the cooling line. For all samples temperature was monitored with a Pt resistor. The 300-K temperature was measured to be nearly constant, without control throughout the data taking at BNL. For the 360-K temperature, monitored and controlled water was circulated through the tubes. A temperature difference occurred at the sample for the maximum stress on, and subsequent stress released, 360 K point, arising from reduced thermal

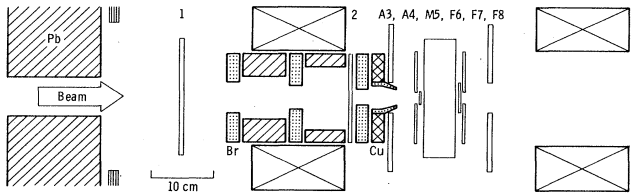

FIG. 2. μSR apparatus used as BNL. A very similar apparatus was used at SIN. The rectangle between the scintillators M5 and F6 represents the cryostat in which the pulling apparatus and sample were placed. The four crossed rectangles are the Helmholtz coils which produced the aligning field.

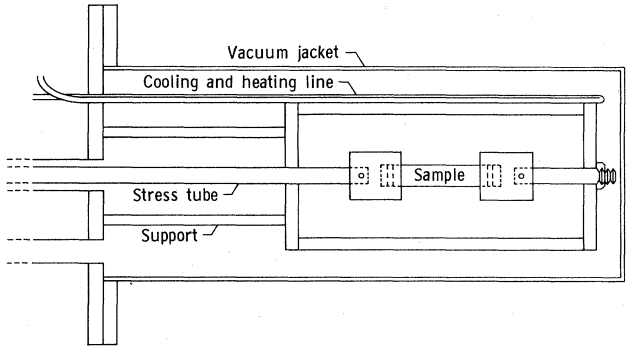

FIG. 3. The pulling apparatus inside a vacuum chamber. The sample shown is the Fe (3 wt. % Si) which was 5 cm long and 1 cm wide. The grooves which were etched into the sample by electrodischarge machining are also indicated.

contact with the Pt resistor associated with melting of the conductive grease. This error was estimated to be 3 K and has been corrected for in plotting the data.

B. Samples

For these experiments we used two single crystal samples. The first (Fe) was nominally pure iron while the second was iron alloyed with 3 wt. % Si. Both samples were supplied by Monocrystals Co. of Cleveland, Ohio.

The Fe single crystal was prepared from a polycrystalline Armco iron ingot which was grown by the strain-anneal method. The sample then was cut using thin abrasive saws and point mills. A chemical etch was used to clean the surfaces and remove surface damage. Final dimensions were $1\times4.6\times46.13$ mm^3, with the $\langle 100\rangle$ along the long axis and the $\langle 010\rangle$, 10° from the flat surface normal. Neutron activation analysis indicates 800 ppm Cu and 500 ppm Mn to be the primary heavy impurities in this sample. The concentrations of C and O were not determined.

The Fe (3 wt. % Si) crystals was grown in vacuum by the Bridgman method from alloy stock which was prepared by intermixing powdered iron (electrolytic grade, 99.52% Fe, 0.04% H, 0.04% C, and 0.05% other) with silicon powder from the Union Carbide Electromet Division. A $\langle 100\rangle$ axis was determined by x-rays and the sample cut and treated by the same techniques used for the pure Fe crystal. Final dimensions were $2.8\times10\times50$ mm^3, the long axis being $\langle 100\rangle$ and the $\langle 010\rangle$ axis 14° from the wide-surface perpendicular. To facilitate pulling, especially at elevated temperatures, grooves 2 mm wide and 1 mm deep were cut in the wide surfaces 2 mm from the ends of the sample using an electrodischarge milling machine.

C. Strain measurements

Strain was induced in the sample by uniaxial stress along the $\langle 100\rangle$ direction applied by a piston and compressed air arrangement for the pure Fe experiment and by dead weights for the Fe (3 wt. % Si) sample. At 300 K the strain was directly measured using a strain gauge. For 360 K the strain was inferred from the stress and elastic constant, which later was obtained by reducing our 300-K constant by the ratio of elastic constants at 360 and 300 K of Ref. 10. Table I shows our values of strain.

D. Data analysis

We used the model functions,

$$N_{F,B}(t)=N_{0_{F,B}}e^{-t/\tau_\mu}\times\{1\pm p[F_l e^{-t/T_1}+F_t e^{-t/T_2}\cos(\omega_\mu t+\phi)]\}+B_{F,B}\ ,$$

which include the effects of longitudinal as well as transverse domain polarization. $p=AP(t=0)$, where A is the effective asymmetry associated with the forward or backward detectors and energy spectrum of the positrons which are detected, and $P(t=0)$ is the muon polarization just after stopping in the sample. The parameters F_t and F_l refer to the fraction of domains which are magnetized transversely and longitudinally, i.e., parallel, to the initial muon polarization.

In the actual fitting process, F_l was factored out of the bracket and F_t replaced by $\beta=F_t/F_l$, which corresponds to the ratio of volumes of domains perpendicular and parallel to the initial muon-spin orientation. The forward and backward histograms of each run were analyzed simultaneously using one value for each parameter which, in principle, would be the same in both histograms. In cases for which T_2 was short, e.g., with cold-worked Fe, replacing e^{-t/T_2} by $e^{-\sigma^2t^2}$ significantly reduced χ^2.

E. Domain alignment with field

For the pure iron sample, surface muons were used which stopped within about 0.1 mm of the surface of the sample. The sample had some surface irregularities and these in turn caused two problems: The domains near the surface were not naturally completely aligned along the long $\langle 100\rangle$ axis; and there was a spatial inhomogeneity to the field.

Since the effect of stress is dependent on the orientation of the domain alignment with respect to the stress axis, several tests were made to verify that the working field was sufficient to bring the sample to essential saturation and domain alignment. Figure 4 indicates the μ-precession frequency as a function of applied field. As one can see, the field penetrates above about 120 Oe for the pure iron sample and 350 Oe for the Fe (3 wt. % Si) sample. The precession frequency drops as a function of external field. This is due to the fact that the internal field is oppositely directed to that of the external field. A demagnetizing field of about these values is expected for ellipsoids of dimension just inscribable in the rectangular

TABLE I. Strain along [100] direction.

Weight (kg)	ϵ_{xx} (microstrain) 300 K	360 K
29.5	82.4	78.6
59.2	169.6	161.9

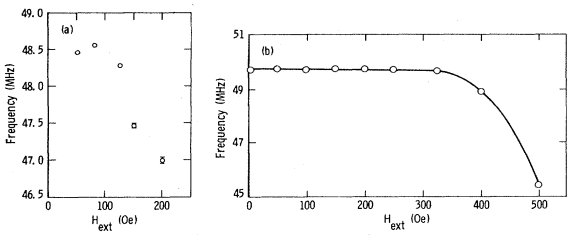

FIG. 4. Muon-precession frequency or (a) the Fe sample at 302 K and (b) the Fe (3 wt. % Si) sample at 300 K as a function of field applied along their long axes. Subsequent stress measurements were done using (a) 150 Oe or (b) 325 Oe.

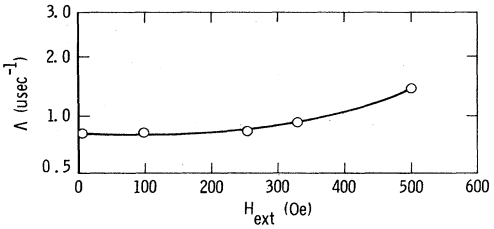

FIG. 6. The depolarization rate Λ for the Fe (3 wt. % Si) as a function of applied field along its long axis. $P(t)=\exp(-\Lambda^2 t^2)$.

samples. We also calculated the penetrating fields based on homogeneously magnetizeable rectangular samples. These are in rough agreement with the frequency fall-off.

A more direct measure of domain alignment is the ratio F_t/F_l. While F_t includes domains not only along $\mathbf{B}_{ext}$, i.e., along the long axis of the sample, but also those transverse to that and the beam, i.e., longitudinal direction, it should be dominated by the domain fraction parallel to $\mathbf{B}_{ext}$. For perfect domain alignment F_t/F_l goes to ∞. In Fig. 5 we can see for pure Fe that above $\mathbf{B}_{ext}=120$ G this ratio is very large and thus we can again conclude that there is essentially complete domain alignment. The principal set of data on pure Fe was taken at 150 G.

For the Fe (3 wt. % Si) sample, for which we used the more uniformly stopping muons of the AGS decay beam, F_t/F_l was always very high and independent of applied field. This clearly indicates that for this sample the domains were always predominantly aligned along the ⟨100⟩ axis parallel to the long axis of the sample, a result expected on energy grounds. For this sample we carried out the stress measurements at 325 Oe. At higher fields where the sample becomes completely magnetized the nonellipsoidal shape produces some field inhomogeneities which are reflected in the depolarization rate increase seen in Fig. 6. Thus by staying at 325 Oe we were able to achieve better frequency accuracy.

III. RESULTS

In Fig. 7 we show the observed precession frequencies for muons in (a) pure Fe at 302 K and in (b) Fe (3 wt. % Si) at 300 K and (c) 360 K as functions of strain along the ⟨100⟩ long axes of the samples. To check the reversibility we took stress-relieved data after each stress-applied point and these frequencies are shown along the horizontal lines. For best straight line fits to the measured points, see Table II.

The hypothesis that the stress-relieved points correspond to a constant frequency is consistent with the data so that inelastic history-dependent effects do not seem to enter. That the stress dependence of the frequency for pure Fe and Fe (3 wt. % Si) agree with each other at room temperature clearly indicates that these stress effects are intrinsic and not impurity sensitive.

The better frequency accuracy for the Fe (3 wt. % Si) sample reflects the slower depolarization rate (hence longer time base for that sample), perhaps a result of the more homogeneous fields deeper in the sample which could be probed with the more penetrating decay beam

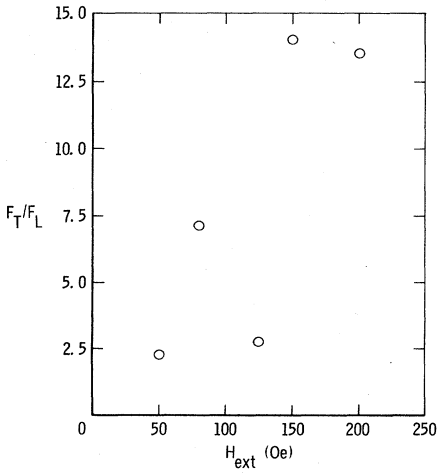

FIG. 5. The ratio F_t/F_l for the Fe sample as a function of field applied along its long axis. F_t/F_l is a measure of domain alignment. Subsequent stress measurements at 150 Oe had nearly complete domain alignment.

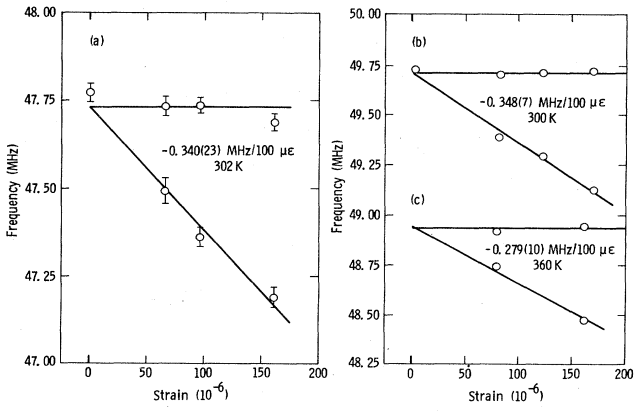

FIG. 7. Muon precession frequencies for (a) Fe at 302 K, (b) Fe (3 wt. % Si) at 300 K, and (c) Fe (3 wt. % Si) at 360 K as functions of strain. The points immediately above the points along the falling straight lines were taken immediately after the lower points and had stress released. That they fall along horizontal lines indicates that we did not encounter irreversible, inelastic effects.

TABLE II. Frequency and field change with strain and temperature.

	Fe 302 K	Fe (3 wt. % Si) 300 K	Fe (3 wt. % Si) 360 K
$\frac{\partial\nu}{\partial\epsilon}$ (MHz)/100 $\mu\epsilon$)	-0.34 ± 0.023	-0.348 ± 0.007	-0.279 ± 0.010
$\frac{\partial B_\mu}{\partial\epsilon}$ (G/100 $\mu\epsilon$)	25.1 ±1.6	25.7 ±0.5	20.6 ±0.7

and also the greater ease with which the alloy sample could be annealed to relieve internal strains at temperatures near melting. In contrast to pure Fe, the alloy here does not undergo the α-γ phase transition, when cooled from the melting point.

Interpretation of the result for $\partial B_\mu/\partial\epsilon$. The derivative of $\mathbf{B}_\mu$, see Eq. (1), with respect to strain, is

$$\frac{\partial\mathbf{B}_\mu}{\partial\epsilon_{100}}=\frac{\partial\mathbf{B}_{\rm ext}}{\partial\epsilon_{100}}+\frac{\partial\mathbf{B}_{\rm dem}}{\partial\epsilon_{100}}+\frac{\partial\mathbf{B}_L}{\partial\epsilon_{100}}+\frac{\partial\langle\mathbf{B}_d\rangle}{\partial\epsilon_{100}}+\frac{\partial\mathbf{B}_{\rm HF}}{\partial\epsilon_{100}}\ .$$

Clearly $\partial\mathbf{B}_{\rm ext}/\partial\epsilon_{100}=0$. The demagnetizing field is on the order of 125 Oe for pure Fe and 325 Oe for (3 wt. % Si) and its fractional change with strain should be on the order of the strain, and thus for 100 $\mu\epsilon$ should only be about 0.01 G and can be ignored.

$\mathbf{B}_L$, the cavity field, is $(4\pi/3)\mathbf{M}_s$, where $\mathbf{M}_s$ is the saturation magnetization. As far as we known, no direct measurement of $\partial M_s/\partial\epsilon$ for a pure Fe crystal has been reported so we consider the following equation:[11]

$$\left[\frac{\partial\lambda_s}{\partial H}\right]_{\sigma,T}=\left[\frac{\partial M_s}{\partial\sigma}\right]_{H,T}\ ,$$

where λ_s is the saturation magnetostriction along the external field H. From the measurement of Calhoun and Carr,[12] $(\partial\lambda_2/\partial H)_{\sigma,T}=2.3\times10^{-10}$/G along the $\langle100\rangle$ axis of a pure Fe crystal at room temperature. Therefore, we obtain $(\partial M_s/\partial\sigma)_{H,T}=2.3\times10^{-4}$ G/bar, which gives $\Delta M_s\cong0.03$ G for $\epsilon_{100}=100$ $\mu\epsilon$. Hence the contribution of $\partial B_L/\partial\epsilon_{100}$ will be neglected.

In the Introduction we said that $\partial\mathbf{B}_{\rm HF}/\partial\epsilon_{100}$ is small. We now justify that statement in more detail.

The hyperfine field at the muon is usually written as

$$B_{\rm HF}=\frac{-8\pi}{3}\eta_{(0)}(\eta_0^+-\eta_0^-)\mu_B\ ,$$

where $\eta_{(0)}$ represents the spin density enhancement produced by the positive charge of the muon and $(\eta_0^+-\eta_0^-)$ is the intrinsic local-spin density at the muon site. We ignore differences in hyperfine fields from one magnetically inequivalent site to another as there is no direct origin for such differences and they would in any case be multiplied by the strain, a small number. The changes in hyperfine field induced by uniaxial strain then must arise from the dependence on the radial distances from nearby Fe atoms. We use the homogeneous pressure results of Butz *et al.*[3] to make estimates for the derivative in two ways: first, by comparing local density changes, and second, by assuming the effect is dominated by nearest neighbors only.

According to Butz *et al.*, $\Delta B_{\rm HF}\approx-3$ G for a positive volume strain of 300×10^{-6} in Fe. The corresponding value of $\Delta M_s=0.234$ G can be obtained by combining the experimental results of $\partial\ln M_s/\partial p=-0.28\times10^{-3}$/kbar and $\partial\ln V/\partial p=-0.59\times10^{-3}$/kbar. Since the change in $(\eta_0^+-\eta_0^-)$ follows roughly that of M_s, we estimate the change in $B_{\rm HF}$ by uniaxial stress to be -0.4 G for 100 $\mu\epsilon$.

Now assuming NN dominance we calculate for octahedral occupancy (the alternative tetrahedral occupancy would have a very small change with stress). Under uniaxial strain the average change in $\mathbf{B}_{\rm HF}$ due to the two nearest-neighbor (NN) atoms, which are half a lattice constant, $(a/2)$ away, is

$$\left\langle\frac{\partial B_{\rm HF}}{\partial\epsilon_{100}}\right\rangle_u=2\frac{\partial B_{\rm HF}}{\partial Z}\frac{a}{2}-4\frac{\partial B_{\rm HF}}{\partial Z}\frac{a}{2}\frac{1}{\rho}\ .$$

The first term arises from sites with tetragonal axis parallel to the stress axis. $\rho=2.74$ is the Poisson ratio for Fe corresponding to the transverse contraction associated with longitudinal elongation. For a strain of say $\epsilon_{100}=100$ $\mu\epsilon$ this leads to

$$\langle\Delta B_{\rm HF}\rangle_u=a\epsilon_{100}\frac{\partial B_{\rm HF}}{\partial Z}\left[1-\frac{2}{\rho}\right]\ .$$

The homogeneous pressure case yields

$$\langle\Delta B_{\rm HF}\rangle_h=a\frac{\Delta V}{V}\frac{\partial B_{\rm HF}}{\partial z}\ ,$$

and, since a 300 $\mu(\Delta V/V)$ corresponds to a 100 $\mu\epsilon$, we have

$$\langle\Delta B_{\rm HF}\rangle_u=\left[1-\frac{2}{\rho}\right]\frac{1}{3}\langle\Delta B_{\rm HF}\rangle_h\ .$$

This results in a -0.27 G per 100 $\mu\epsilon$ shift. This is even smaller than the first estimate and in both cases $\partial B_{\rm HF}/\partial\epsilon_{100}$ is small enough to be neglected.

Thus we are left with only $\partial\langle B_d\rangle/\partial\epsilon_{100}$ as the dominant contribution for $\partial B_\mu/\partial\epsilon_{100}$. The change in $\langle B_d\rangle$ by uniaxial stress arises from two effects. First, there is a change in the muon-occupation probabilities between magnetically inequivalent sites where the signs and magnitudes of B_d are quite different; and second, uniaxial stress lowers the symmetry so that the sum of B_d over the three octa- or tetrahedral sites for an Fe unit cell is not zero anymore. We can combine these contributions to $\langle B_d\rangle$ as

$$\langle B_d\rangle=+\tfrac{2}{9}(B_l-B_t)(\Delta E/kT)+\tfrac{1}{3}(B_l+2B_t)\ , \qquad (2)$$

where

$$\Delta E=-\frac{(S_{11}-S_{12})}{S_{11}}(P_1-P_2)\epsilon_{100}$$

TABLE III. Magnetic dipolar fields under various conditions at $T=0$ K.

	Site	
	$4T(O)$	T
(1) Pointlike muon, rigid lattice	18.5	−5.2 kG
(2) Pointlike muon, nearest neighbors relaxed according to scaling from Nb and V	13.5	−3.7 kG
(3) Spherical muon wave function $\alpha=\beta=0.15-0.19$ lattice relaxed as in (2)	13	−3.7 kG
(4) Oblate muon wave function to match the general shape of a muon in Nb and V, $\alpha=0.19$, $\beta=0.15$	9.3	
(5) Prolate muon wave function to match the T site shape in Nb and V, $\alpha=0.19$, $\beta=0.25$		−4.8 kG
(6) Pointlike muon, lattice relaxed as in the calculations of Jena *et al.*	11.2	−4.4 kG
(7) Muon wave function as calculated by Jena *et al.*, lattice relaxed as in (6) $B_{\rm dip}(T)=B_{\rm dip}(0)M_s(T)/M_s(0)$ $M_s(O)=1.750$ kG $M_s(300\ {\rm K})=1.688$ kG $M_s(360\ {\rm K})=1.658$ kG	7.6	−4.4 kG
(8) $\delta(B_l+2B_t)/100\ \mu\epsilon$		
Pointlike muon	−7.1	−2.3 G/100 $\mu\epsilon$
Calculated muon wave function and lattice relaxed	−2	−1 G/100 $\mu\epsilon$

is the difference in free energies between the magnetically inequivalent sites, the S_{ij} are elastic constants, and P_i are diagonal elements of the double force tensor for the muon in Fe. For the case at hand, with strain along a $\langle 100\rangle$ axis, the second term is negative and less than 5 G in magnitude for $\epsilon_{100}=100\times10^{-6}$ at either the octa- or tetrahedral sites. The sign of the first term, from our calculations, is positive and dominates, accounting for the decrease in magnitude of $\mathbf{B}_\mu$. Estimates for B_l and B_t are dependent upon the lattice site, the local lattice distortion due to the presence of the muon, the shape and symmetry of the muon wave function, and upon changes in nearby iron moments produced by the muon. For a pointlike muon in an undistorted, unstrained lattice of unperturbed Fe moments B_l ($B_t=-\frac{1}{2}B_l$ here) is 18.5 (−5.21) kG at octahedral (tetrahedral) sites.

If we use the displacements of lattice ions calculated by Sugimoto and Fukai[5] for the muon in Nb, B_l in Fe reduces to 13.56 (−3.73) kG at octahedral (tetrahedral) sites for a pointlike muon. In the $\langle B_d\rangle$ calculations, the differences in elastic properties between Fe and Nb enter only in second order and will be ignored.

For a short-ranged, spherically symmetric muon probability-density distribution the averaged B_l will be the same as for a pointlike muon at the site. However since the local site has only tetragonal symmetry we will take the form of the muon distribution as

TABLE IV. P_1-P_2 for the double-force tensor.

Site	P_1-P_2 (eV) 3.3 Å	2.87 Å
$4T(O)$	3.466	3.73
$1T$	−1.075	−1.23

$$|\psi_\mu(\mathbf{r})|^2=\frac{1}{\alpha^2\beta\pi^{3/2}}\exp\left[-\frac{x^2+y^2}{\alpha^2}-\frac{z^2}{\beta^2}\right],$$

for the site with the tetragonal axis parallel to $\mathbf{M}_s=M_s\hat{Z}$. Comparing the shape of the Gaussian-type wave function and those calculated by Sugimoto and Fukai for Nb, we estimate the value of α to be around 0.2 in units of the lattice parameter. Calculations have been performed varying α from 0.15 to 0.25 for the $4T(O)$ octahedral site, and from 0.15 to 0.22 for the tetrahedral site. Geometric considerations suggest $\alpha\approx\sqrt{2}\beta$ for the $4T(O)$ site and $\alpha\approx(1/\sqrt{2})\beta$ for the $1T$ site.

Jena *et al.*[6] have calculated muon wave functions and lattice displacements specific to the case of a muon in Fe. They also calculated the dipolar fields appropriate to their results, and these are presented in Table III as well as the change in $\frac{1}{3}(B_l+2B_t)$ induced by strain.

Now to see whether Eq. (2) is correct in the sense that the dominant effect which comes from the first term has the expected temperature dependence. We subtract the small final term from δB_μ obtaining:

$$\delta B'_\mu=+\tfrac{2}{9}(B_l-B_t)\Delta E/kT=\delta B_\mu-\tfrac{1}{3}(B_l+2B_t)\ .$$

The left side is proportional to $M_s(T)/T$, the saturation magnetization divided by the temperature. We thus expect that between 300 and 360 K, a ratio of $[M_s(300)/300]/[M_s(360)/360]=1.22$, while the right-side ratio, using a weighting of 1:2 for octahedral to tetrahedral occupation, is $(25.7+1.33=27)/(20.6+1.33=21.9)=1.23$, in excellent agreement. Since $B_l\approx-2B_t$, we may write

$$\delta B'_\mu=\tfrac{1}{3}B_l(0\ {\rm K})\frac{M_s(T)}{M_s(0\ {\rm K})}\frac{\Delta E}{kT}\ .$$

TABLE V. $\delta B'_\mu$ in Gauss for room temperature, calculated under various conditions. The average is for 1:2 weights for the $4T(O)$:$1T$ sites.

	$4T(O)$		$1T$		Average
	$\delta B'_\mu$ G/100 $\mu\epsilon$	ΔE (meV)	$\delta B'_\mu$ G/100 $\mu\epsilon$	ΔE (meV)	$\delta B'_\mu$ G/100 $\mu\epsilon$
Jena *et al.*[a]	18	0.19	29	−0.53	25.3
Extrapolate ΔE from Nb and V (see footnote b below) fields from (7) of Table III.	61	0.51	10.5	−0.17	27.3
Extrapolate ΔE from Nb and V (see footnote b below) fields from (4) and (5) of Table III.	50	0.51	9.6	−0.17	23.0
Reversal of ΔE from Jena *et al.*[a]	51.8	0.53	10.7	−0.19	24.4
Experiment corrected for the small effects of dipole motion using results of Jena *et al.*[a]					27±.5

[a]Reference 6.
[b]Reference 5, also see text.

Jena *et al.* have obtained $\Delta E = -0.19$ and $+0.53$ meV for the $4T(O)$ and $1T$ sites, respectively. Using these they obtain 18 and 29 G/100 $\mu\epsilon$ for the two sites. If again we assume equal occupation of these two types of sites, weighting them as 1:2 we obtain for the average shift 25.3 G/100 $\mu\epsilon$ which is certainly very close to the observed result of 27±0.5 G/100 $\mu\epsilon$.

We can also extrapolate the results of Sugimoto and Fukai[5] on Nb and V to find the double force tensor diagonal elements for Fe in the two different types of sites. The extrapolation was linear in the lattice parameter observing that $P_1 - P_2$ changed by 5.3% and 9.7% for the $4T(O)$ and $1T$ sites, respectively, in their calculations upon decreasing the lattice parameter from 3.3 Å to 3.0 Å and then using the 2.87 Å lattice parameter of Fe. (See Table IV.)

Since $\Delta E = [(S_{11} - S_{12})/S_{11}]\,(P_1 - P_2)\epsilon_{100}$, we find that ΔE is −0.51 meV for the $4T(O)$ site and 0.17 meV for the $1T$ site. Using this ΔE and $B_l(0)$ which we calculate [9.3 kG for the $4T(O)$ site and −4.8 kG for the $1T$ site] we obtain the $\delta B'_\mu$ shown in Table V. We also include the results for the fields calculated by Jena *et al.* Since it is rather surprising that ΔE for the $4T(O)$ site is smaller in magnitude than that for the $1T$ site in the calculations of Jena *et al.*, we finally present the results obtained upon reversing the ΔE though keeping the physically reasonable signs.

IV. CONCLUSIONS

We have determined that the precession frequency as a function of uniaxial strain for Fe arises primarily from symmetry breaking effects. The magnitude of the shift is reasonably well described by either the results of Jena *et al.*[6] or by extrapolation from the results of Sugimoto and Fukai[5] for Nb and V if one assumes in both cases that the muon occupies nearly equally the $4T(O)$ and $1T$ sites. This last is consistent with the results of Yagi *et al.*[7] and with the calculations for the energies of these sites, which are nearly equal. To be precise there is about a 30-meV difference favoring the $4T(O)$ site in the calculations, but this is thought by Jena *et al.*[6] not to be significant.

The reduction of precession frequency with extension along ⟨100⟩ magnetization directions can explain the tendency for cold-worked iron samples to have reduced precession frequencies. Since magnetostriction in Fe favors domain alignment along the local directions of extension, the average precession frequency should thus be reduced.

That depolarization rates are evidently sensitive to internal strains and that these will become more important at lower temperatures imply that interpretations of depolarization rates which do not take these effects into account may need reevaluation.

Similar frequency shifts associated with symmetry breaking should occur for those crystalline materials such as Fe_3Si or Fe_3Al which also have crystallographically equivalent potential muon sites which are magnetically inequivalent. Other systems, such as Ni, Co, or Gd, though having only one type of site, should have observable, if smaller, frequency shifts arising from the motion with stress of the crystal atoms and their associated dipole and hyperfine field distributions. The effects of working the Fe samples which show up in irreversible frequency shifts, usually toward lower values, and depolarization rate increases, have only been partially explored so far and will be reported later.

ACKNOWLEDGMENTS

We would like to thank P. Jena and K. Petzinger for helpful discussions. This work was supported in part by National Science Foundation (NSF) Grant DMR-8007059 and National Aeronautics and Space Administration (NASA) Grant Nos. NSG 1342 and NAG1-416.

*Current address: NASA Langley Research Center, Hampton, VA 23665.

[1]P. F. Meier, Hyperfine Interact. **8**, 591 (1981).
[2]K. Kanamori, H. Yoshida, and K. Terakura, Hyperfine Interact. **8**, 573 (1981).
[3]T. Butz, J. Chappert, J. F. Dufresne, O. Hartmann, E.

Karlsson, B. Lindgren, L. O. Norlin, P. Podini, and A. Yaouanc, Phys. Lett. **75A**, 321 (1980).
[4]H. Kanzaki, J. Phys. Chem. Solids **2**, 24 (1957).
[5]H. Sugimoto and Y. Fukai, Phys. Rev. B **22**, 760 (1980).
[6]P. Jena, M. Manninen, R. M. Nieminen, and J. J. Puska, Phys. Rev. B **29**, 4170 (1984).
[7]E. Yagi, G. Flik, K. Furderer, N. Haas, D. Herlach, J. Major, A. Seeger, W. Jacobs, M. Krause, H.-J. Mundinger, and H. Orth, Phys. Rev. B **30**, 441 (1984); E. Yagi, H. Bossy, K.-P. Döring, M. Gladisch, D. Herlach, H. Matsui, H. Orth, G. zu Putlitz, A. Seeger, and J. Vetter, Hyperfine Inter. **8**, 553 (1981).
[8]R. A. Johnson, G. J. Dienes, and A. C. Damask, Acta Metall. **12**, 1215 (1964).
[9]C. E. Stronach, K. R. Squire, A. S. Arrott, B. Heinrich, W. F. Lankford, W. J. Kossler, and J. J. Singh, in *Electronic Structure and Properties of Hydrogen in Metals,* edited by P. Jena and C. B. Satterthwaite (Plenum, New York, 1983), p. 617, and references therein.
[10]J. Leese and E. Lord, J. Appl. Phys. **39**, 8 (1968).
[11]A. H. Morrish, *The Physics Principles of Magnetism* (Wiley, New York, 1965).
[12]W. J. Carr, Jr., in *The Encyclopedia of Physics* (Springer, Berlin, 1966), Vol. XVIII/2, p. 308.